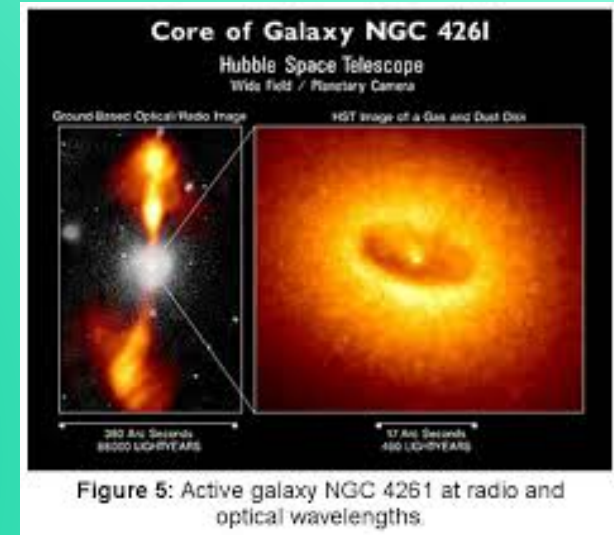
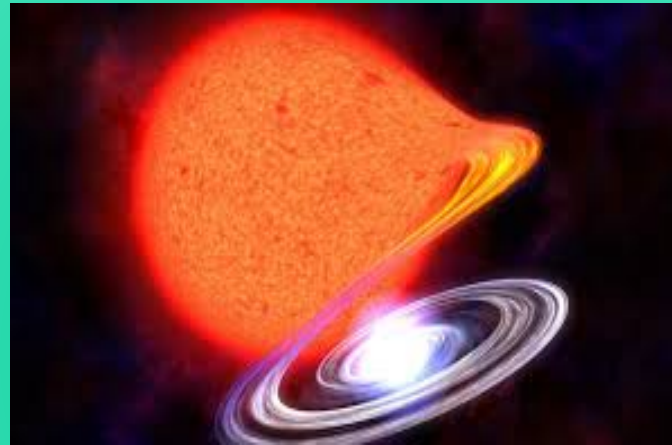
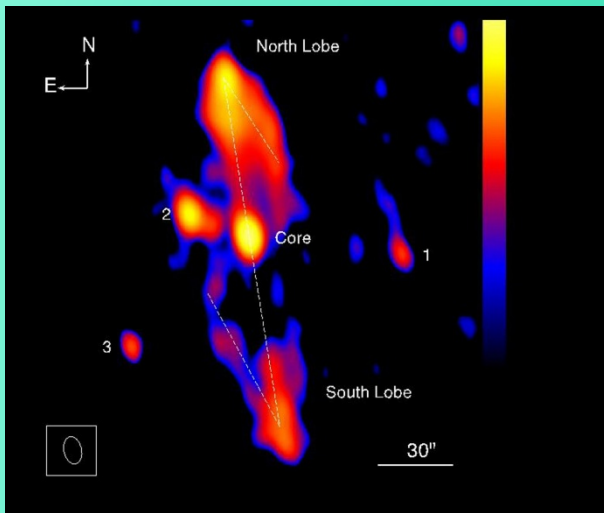


# Relativistic Jets from black hole (BH) accretion disc

Artist's view NS Xray binary



GRS 1758-258, Nature '17

AGN, NGC 4261

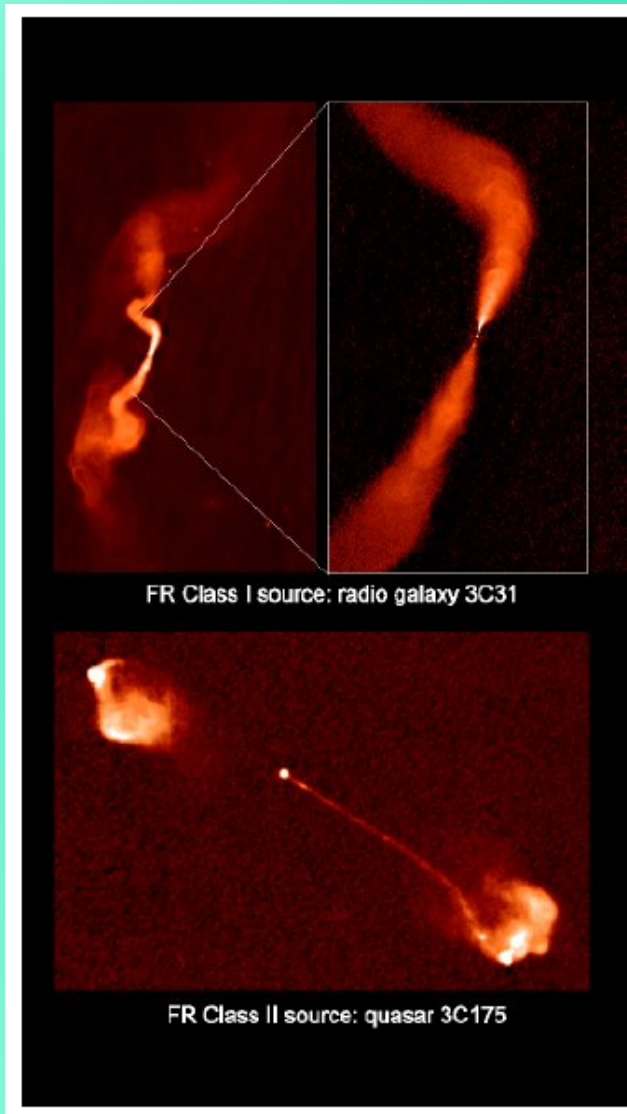
HEPRO-VII, Univ. de Barcelona, 9-12 July, 2019

Indranil Chattopadhyay

Aryabhata Research Institute of observational sciencES

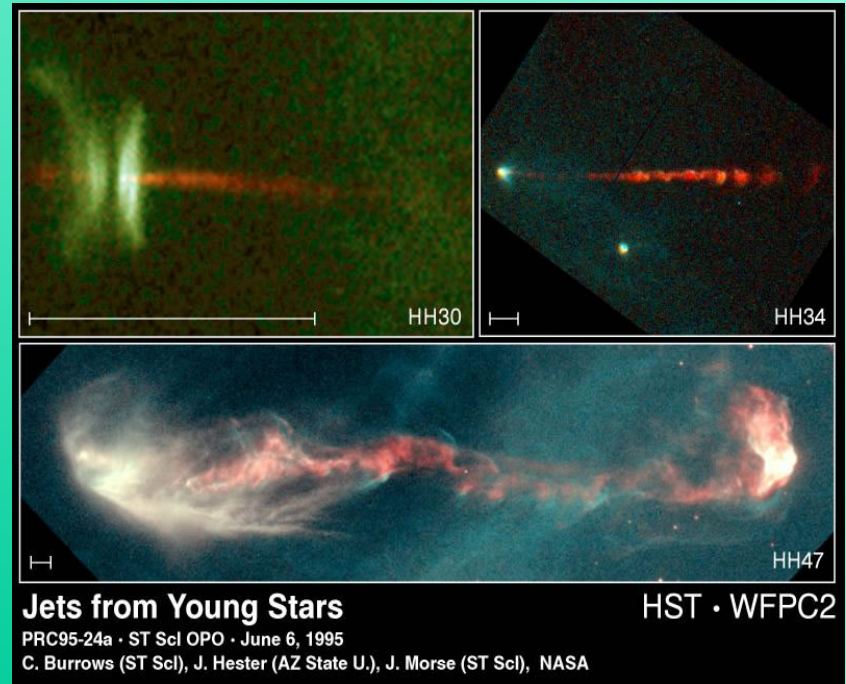
indra@aries.res.in

# Jets are ubiquitous



AGN

YSO



Micro-Quasar GRO J 1655-40

Jets around black hole is potentially relativistic.

□ Properties of jet:

(i) Terminal speeds are inferred to be relativistic.

(ii) Jets are collimated (few less than others though)

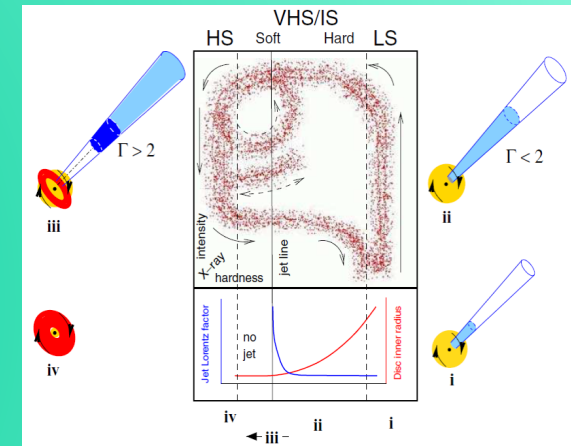
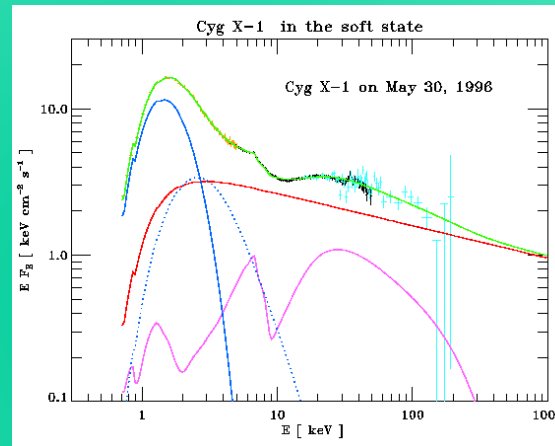
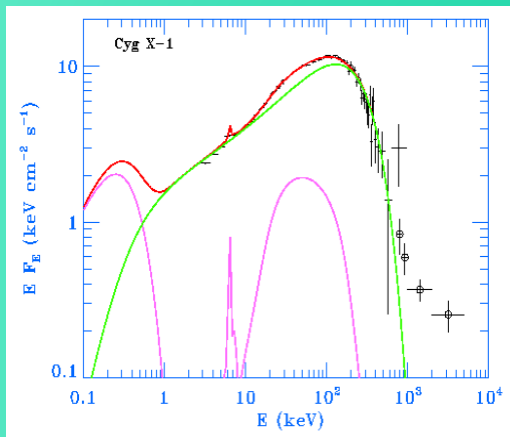
□ Things not known about jets

(i) How jets are formed? BZ process or plasma effects!

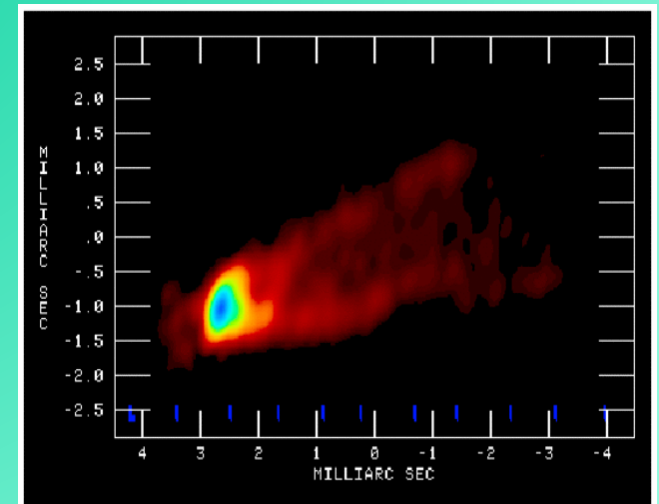
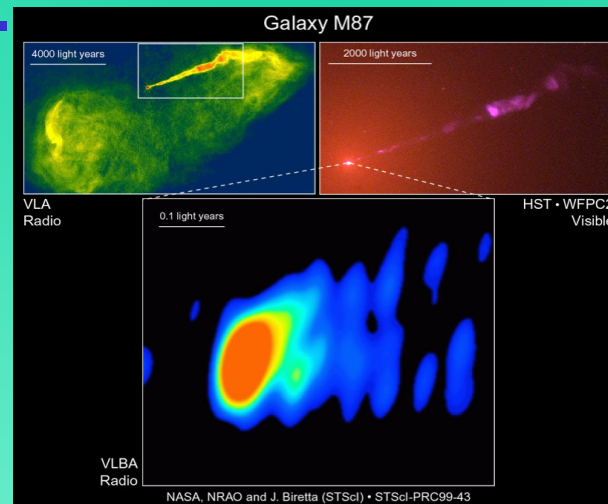
(ii) Composition of the jet.

- There is enough indirect evidence that large scale jet is matter dominated. (Reynolds et al 1996, Romero et al 2016)
- And that jet states are correlated with the accretion states.

Implies accreting matter launches jet (??)



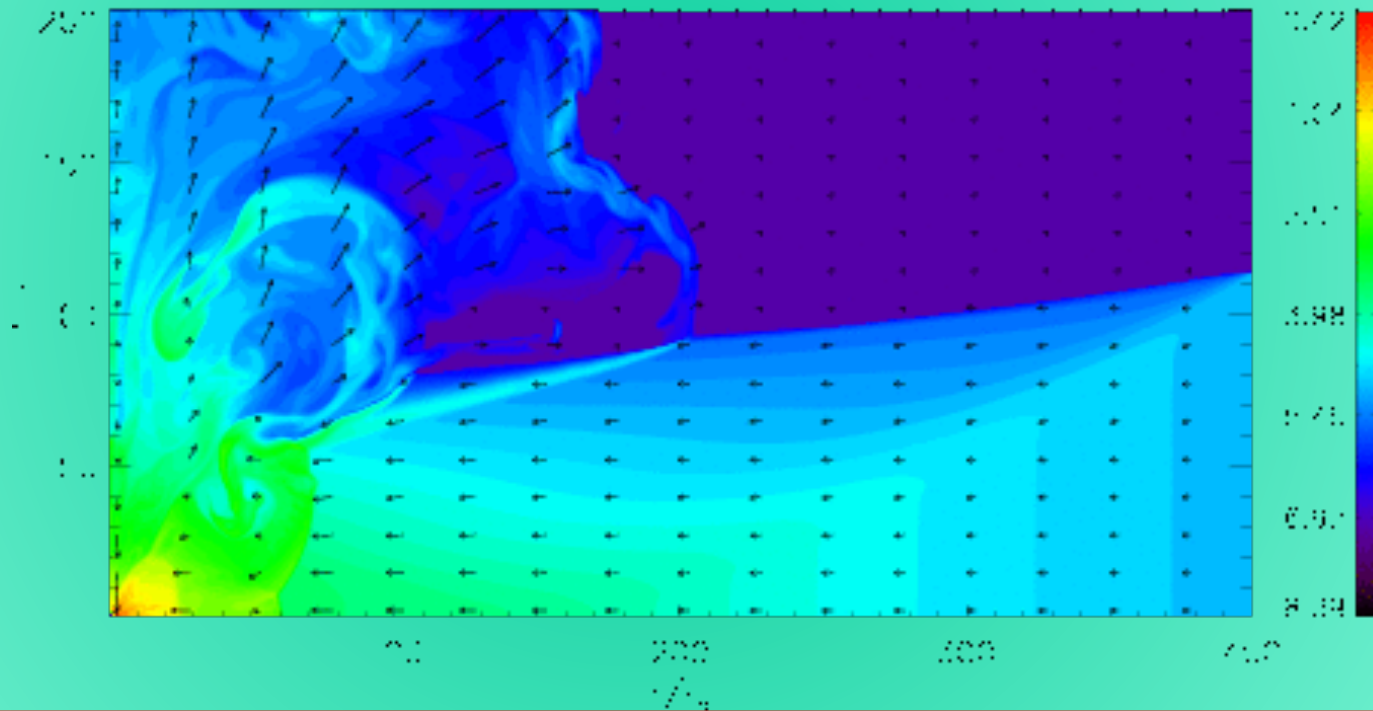
- Moreover, jets appears to be launched from a region close to the central BH.



In addition, the low frequency QPO is also correlated with the jet states.

We have performed some HD simulations which showed general broad agreement with the observations mentioned above.

(Lee, IC et. al. 2016)



However, in this talk, we focus mainly on driving mechanism and composition of jets

Since the observed jet is most certainly matter dominated, we assume the jet originating from a region close to the BH, is also matter dominated at the launch site.

As jet is launched from the accretion disc, it should start with negligible velocity.

If  $E$  is the Bernoulli parameter of the jet, then the terminal speed is ; or

$$E = -hu_t = -h_\infty u_{t\infty} = \gamma_\infty = (1 - v_\infty^2)^{-1/2}$$

$$v_\infty = \left(1 - \frac{1}{E^2}\right)^{1/2}$$

**i.e., to get Lorentz factor of 10,  $E$  has to be 10, i.e., at the base  $\gamma_b \sim 1$ ,  $g_{tt} \sim 0.8$  i.e,  $h_b > 10$  so  $T_b \sim 10^{13}\text{K}$ , such high temperatures are not obtained in realistic accretion discs.**

*Therefore, jets cannot be solely thermally driven*

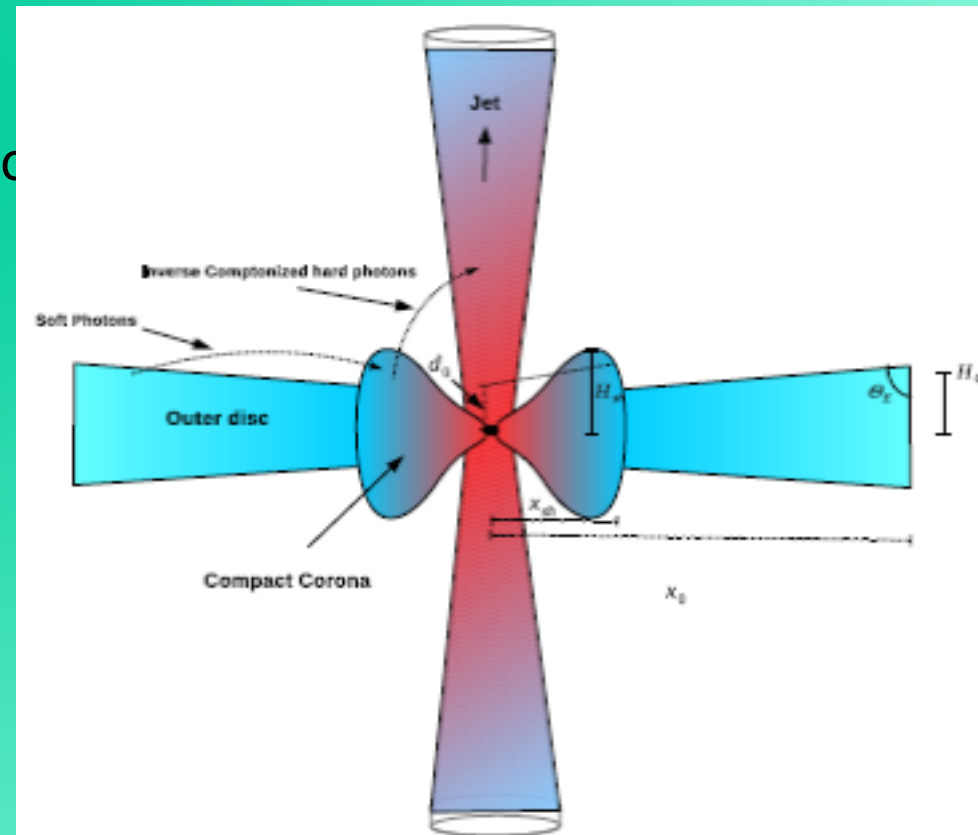
- ❑ Intense radiation field near the accretion disc, may also drive outflowing matter as relativistic jets.
- ❑ However, in presence of high thermal energy, radiation driving tends not to be important, and
- ❑ additionally optically thin jets are subjected to radiation drag.
- ❑ What about collimation?

- ❖ Magnetic field on the other hand, ticks almost all the boxes.
- ❖ Although, the temperature at the jet base are generally too high.
- ❖ It is also intriguing, how the magnetic field configuration change with the spectral state change, to enable the jet states to be correlated to the accretion disc spectral states.

We investigate whether (i) outflows can be accelerated to relativistic speed and whether (ii) if magnetic field do the same. Moreover, does composition have any effect on the solutions of the outflows.

### I. Radiatively Driven Jets:

- Inner disc is like a torus (may be due to shock or radiation pressure supported or both).
- Outer disc also has advection term (moments from  $Kep$  disc is much smaller)
- Both are source of radiation.
- Curvature effects are considered.
- Relativistic eq. of state is considered.



We investigate whether (i) outflows can be accelerated to relativistic speed and whether (ii) if magnetic field do the same. Moreover, does composition have any effect on the solutions of the outflows.

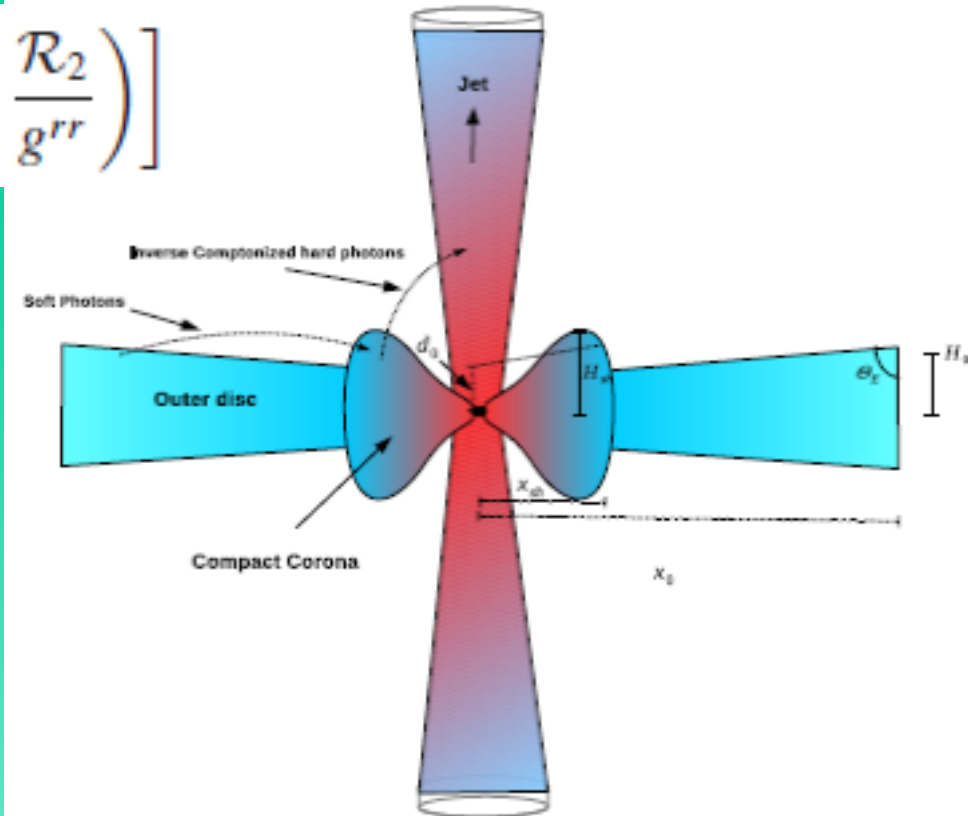
## Governing equations

$$u^r \frac{du^r}{dr} + \frac{1}{r^2} = - \left( 1 - \frac{2}{r} + u^r u^r \right) \frac{1}{e + p} \frac{dp}{dr} + \rho_e \frac{\sqrt{g^{rr}} \gamma^3}{(e + p)} \mathfrak{S}^r$$

I. Radiation

$$\mathfrak{S}^r = \frac{\sigma}{m_e} \left[ (1 + v^2) \mathcal{R}_1 - v \left( g^{rr} \mathcal{R}_0 + \frac{\mathcal{R}_2}{g^{rr}} \right) \right]$$

- Inner shock or radiation pressure supported or both).  $\frac{de}{dr} - \frac{e + p}{\rho} \frac{d\rho}{dr} = 0$
- Outer shock (momenta from Kepler disc is much smaller)
- Both a radiation.
- Curvature effects are considered.
- Relativistic eq. of state is considered.



We investigate whether (i) outflows can be accelerated to relativistic speed and whether (ii) if magnetic field do the same. Moreover, does composition have any effect on the solutions of the outflows?

### I. Radiatively Driven Jets:

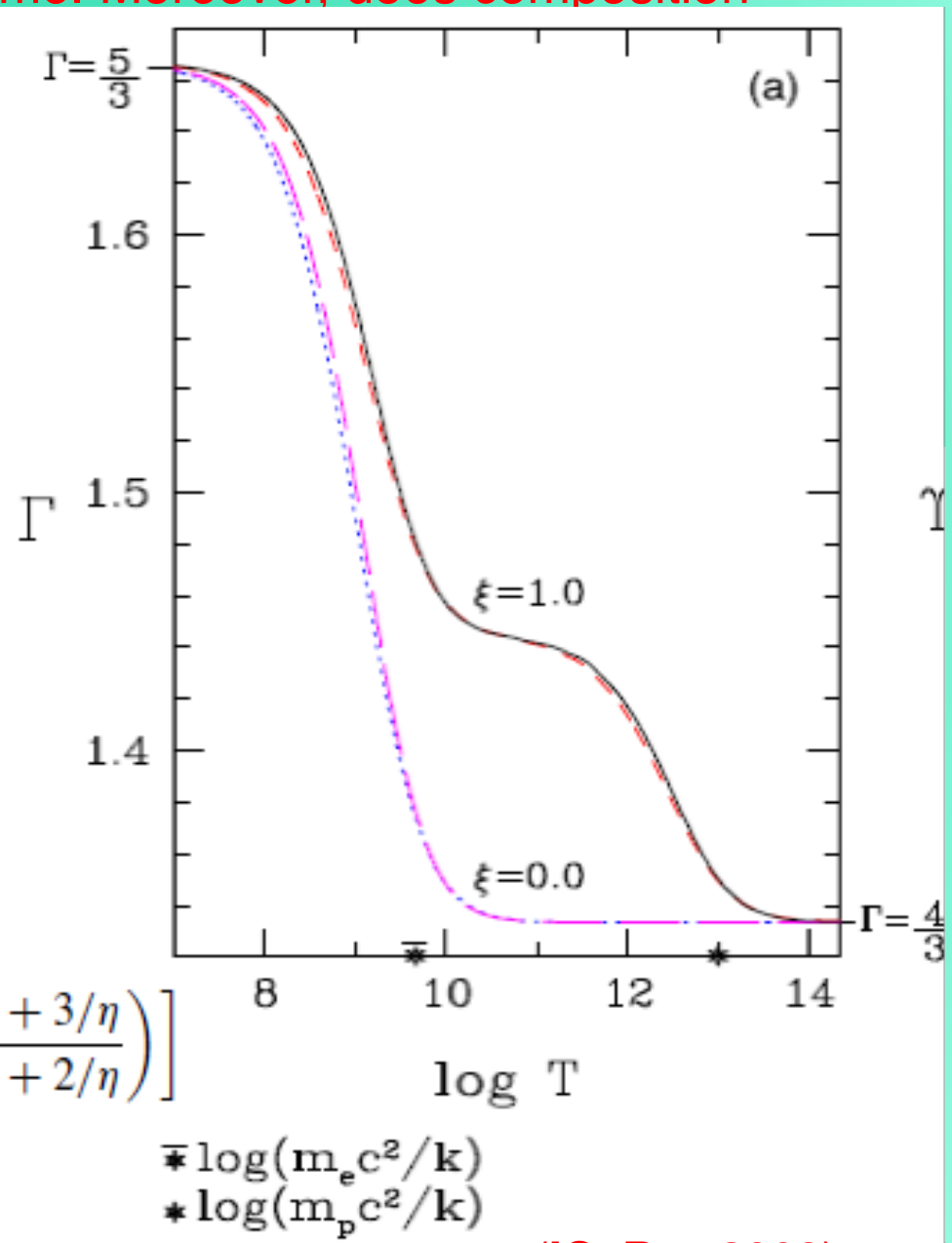
- Inner disc is torus like (may be due to shock or radiation pressure supported or both).
- Outer disc also has advection term.
- Both are source of radiation.
- Curvature effects are considered.
- Relativistic eq. of state is considered (CR EoS)

$$e = n_e m_e c^2 f$$

$$f = (2 - \xi) \left[ 1 + \Theta \left( \frac{9\Theta + 3}{3\Theta + 2} \right) \right] + \xi \left[ \frac{1}{\eta} + \Theta \left( \frac{9\Theta + 3/\eta}{3\Theta + 2/\eta} \right) \right]$$

$$\Theta = kT / (m_e c^2)$$

$$N = \frac{1}{2} \frac{df}{d\Theta}; \quad \Gamma = 1 + \frac{1}{N}$$



(IC, Ryu 2009)

We investigate whether (i) outflows can be accelerated to relativistic speed and whether (ii) if magnetic field do the same. Moreover, does composition have any effect on the solutions of the outflows?

### I. Radiatively Driven Jets:

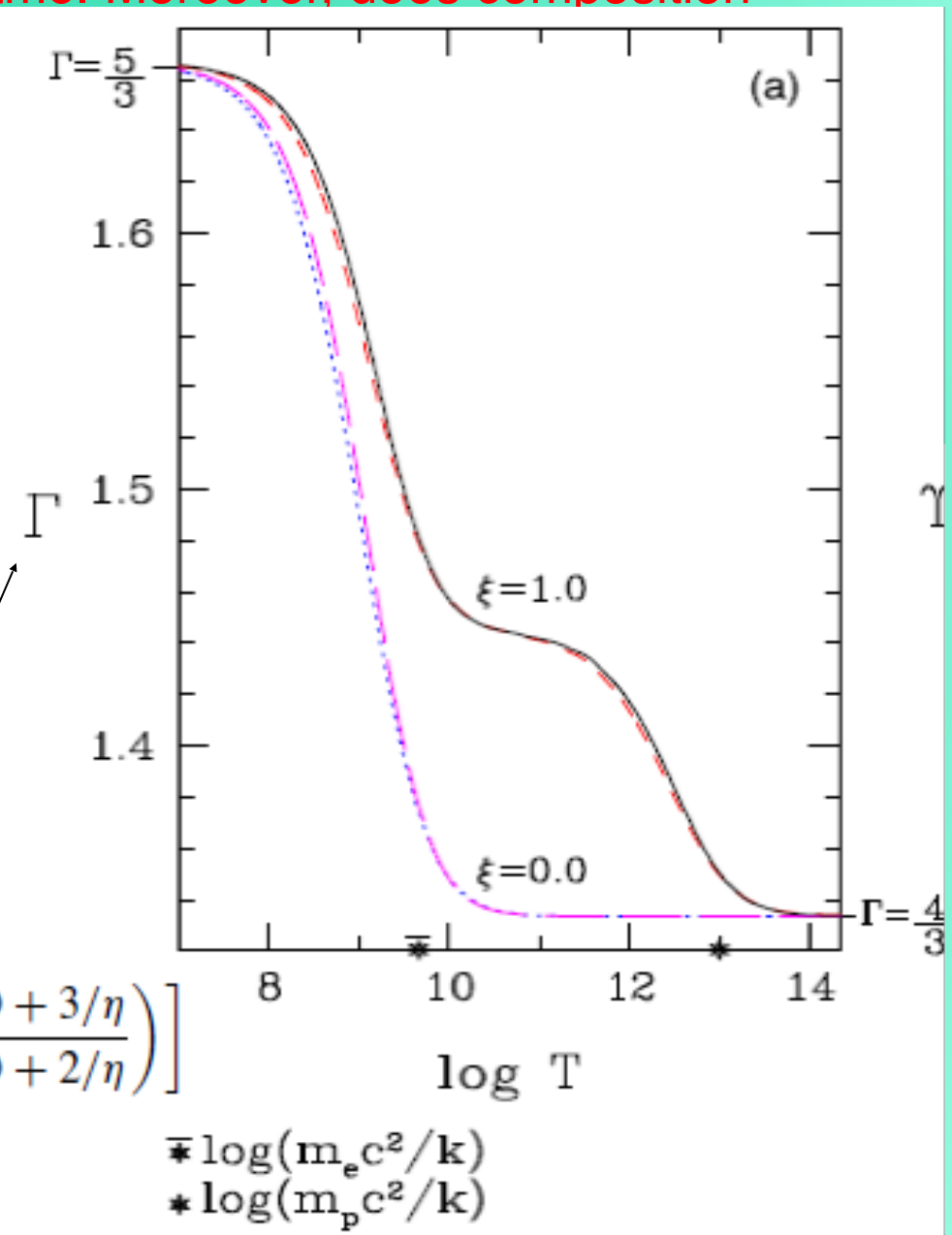
- Inner disc is torus like (may be due to shock or radiation pressure supported or both).
- Outer disc also has advection term.
- Both are source of radiation.
- Curvature effects are considered.
- Relativistic eq. of state is considered (CR EoS)

$$e = n_e m_e c^2 f$$

$$f = (2 - \xi) \left[ 1 + \Theta \left( \frac{9\Theta + 3}{3\Theta + 2} \right) \right] + \xi \left[ \frac{1}{\eta} + \Theta \left( \frac{9\Theta + 3/\eta}{3\Theta + 2/\eta} \right) \right]$$

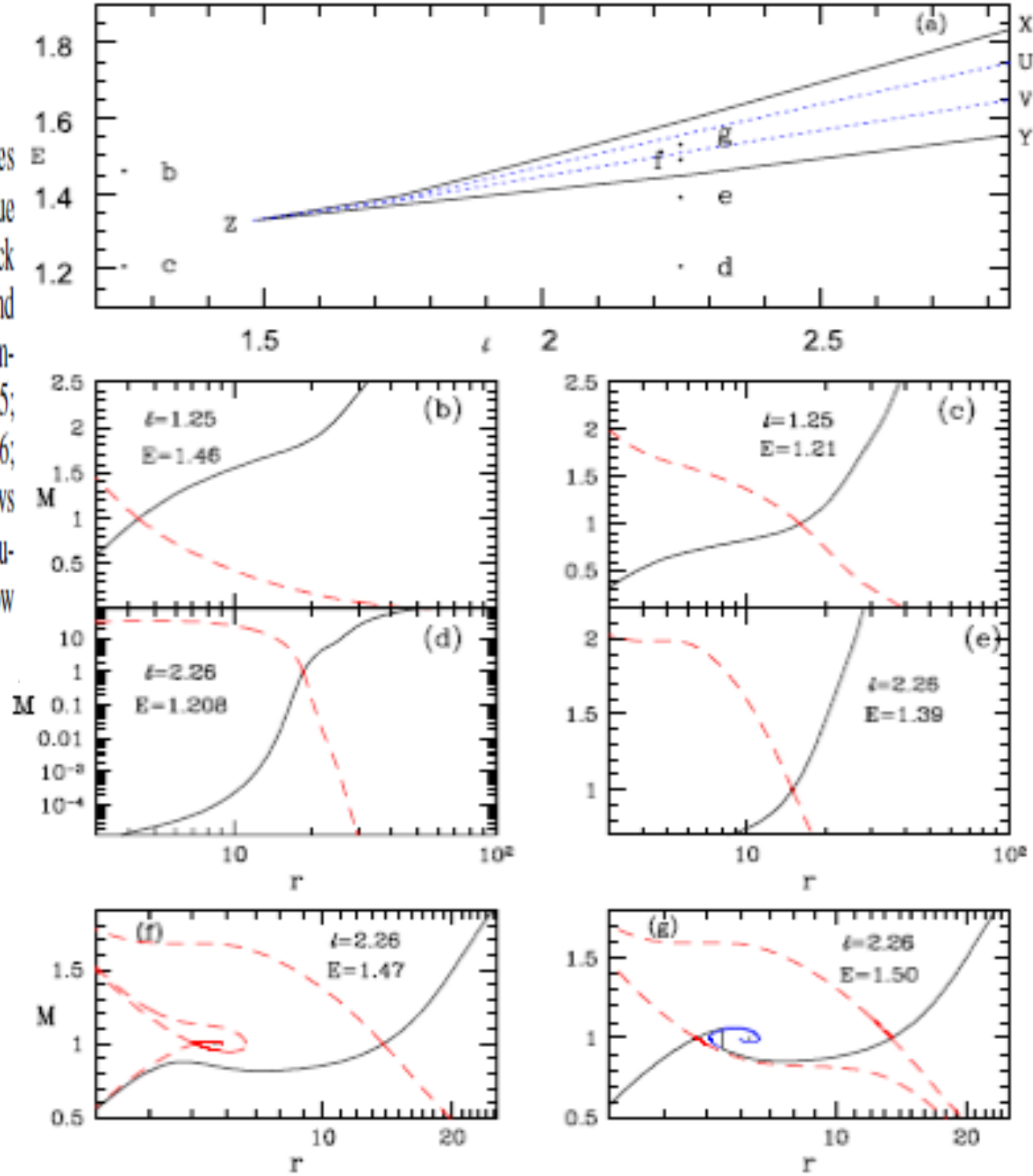
$$\Theta = kT/(m_e c^2)$$

$$N = \frac{1}{2} \frac{df}{d\Theta}; \quad \Gamma = 1 + \frac{1}{N}$$



# Thomson Scattering cross-section

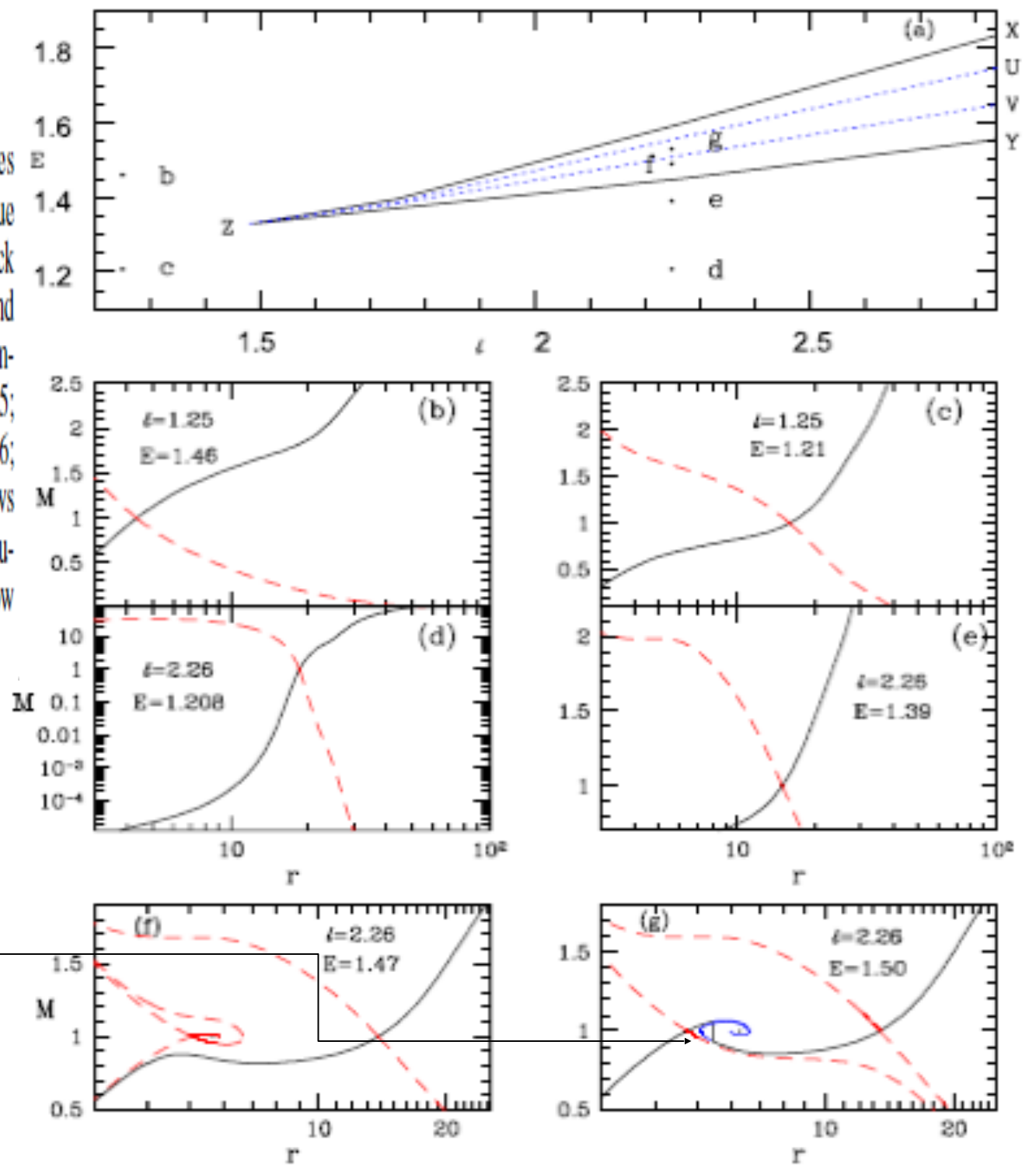
Fig. 8. Panel a:  $E - \ell$  parameter space: bounded region XZY signifies parameters for multiple sonic points in jet and region UZV within blue dotted lines represents parameters for which flow goes through shock transition. Filled circles named "b-g" are the flow parameters  $E$  and  $\ell$ , for which the jet solutions are plotted in panels b-g. Mach number  $M = v/a$  is plotted as a function of  $r$  for b)  $E = 1.46, \ell = 1.25$ ; c)  $E = 1.208, \ell = 1.25$ ; d)  $E = 1.208, \ell = 2.26$ ; e)  $E = 1.39, \ell = 2.26$ ; f)  $E = 1.47, \ell = 2.26$ ; and g)  $E = 1.5, \ell = 2.26$ . Each panel shows physical jet solutions (solid black line) and corresponding inflow solutions (dashed red line). Sonic points are shown by the crossing of inflow and jet solutions. All solutions are for  $e^- - p^+$  flow.



Radiation drag has limited effect in such radiation field.

(Vyas, IC 2018)

**Fig. 8.** Panel a:  $E - \ell$  parameter space: bounded region XZY signifies parameters for multiple sonic points in jet and region UZV within blue dotted lines represents parameters for which flow goes through shock transition. Filled circles named "b-g" are the flow parameters  $E$  and  $\ell$ , for which the jet solutions are plotted in panels b-g. Mach number  $M = v/a$  is plotted as a function of  $r$  for b)  $E = 1.46, \ell = 1.25$ ; c)  $E = 1.208, \ell = 1.25$ ; d)  $E = 1.208, \ell = 2.26$ ; e)  $E = 1.39, \ell = 2.26$ ; f)  $E = 1.47, \ell = 2.26$ ; and g)  $E = 1.5, \ell = 2.26$ . Each panel shows physical jet solutions (solid black line) and corresponding inflow solutions (dashed red line). Sonic points are shown by the crossing of inflow and jet solutions. All solutions are for  $e^- - p^+$  flow.



Radiation drag has limited effect in such radiation field.

Radiatively driven shock

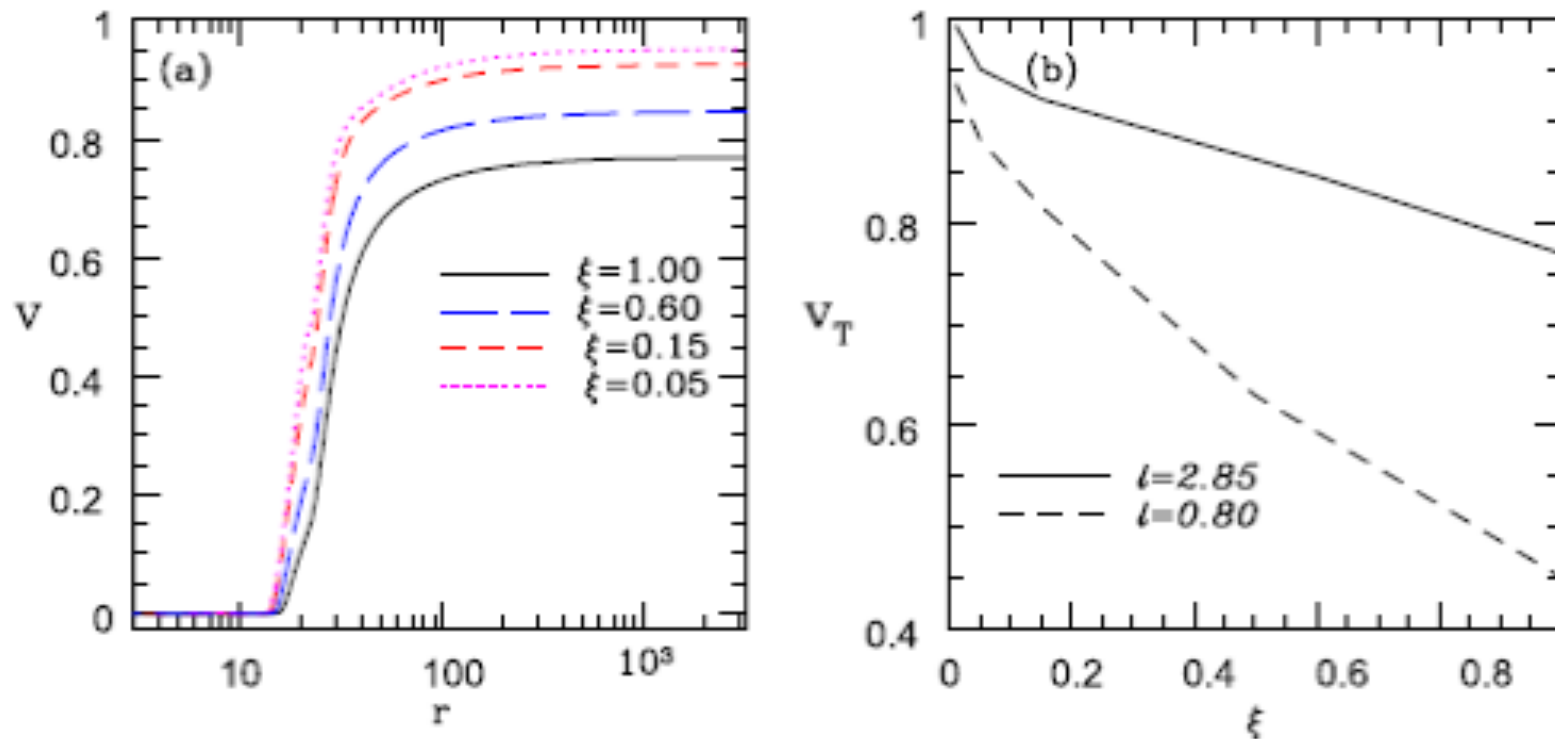


**Fig. 12.** *Panel a:*  $v$  as a function of  $r$  for jets acted on by disc radiation marked by  $\xi = 1.0$  (solid black line);  $\xi = 0.6$  (long-dashed blue line),  $\xi = 0.15$  (dashed red line) and  $\xi = 0.05$  (dotted magenta line). The disc radiation is for  $\ell = 2.85$ . *Panel b:* variation of  $v_T$  with  $\xi$  for “f”-type jets, driven by radiation quantified by  $\ell = 2.85$  (solid line) and  $\ell = 0.8$  (dashed line).

(Vyas, IC 2018)

Pair dominated flow can reach ultra-relativistic speed, however, the temperature at the base of the jet is  $> 10^{12}$  K

In order to rectify this discrepancy, we considered energy exchange through Compton scattering.

$$\sigma = \chi_c \sigma_T = \left[ \frac{1}{1 + \left( \frac{T_e}{4.5 \times 10^8} \right)^{0.86}} \right] \sigma_T$$

Compton cross-section is less than Thomson's... But there is energy transfer... Could the lack of momentum transferred be compensated by energy transfer??

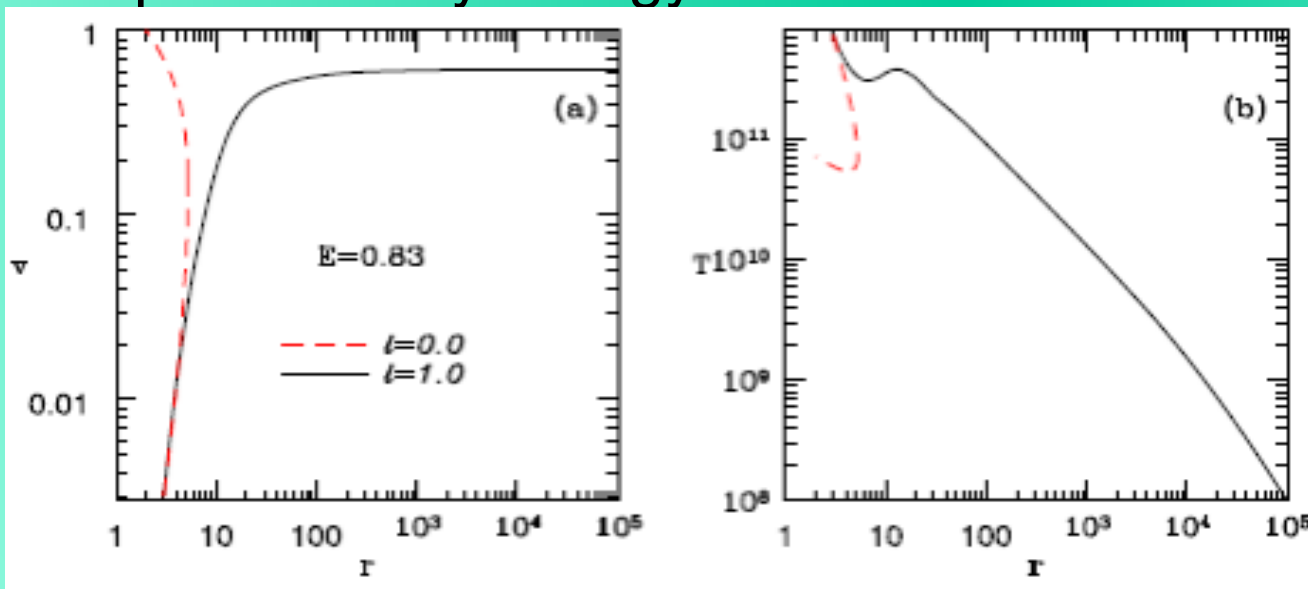
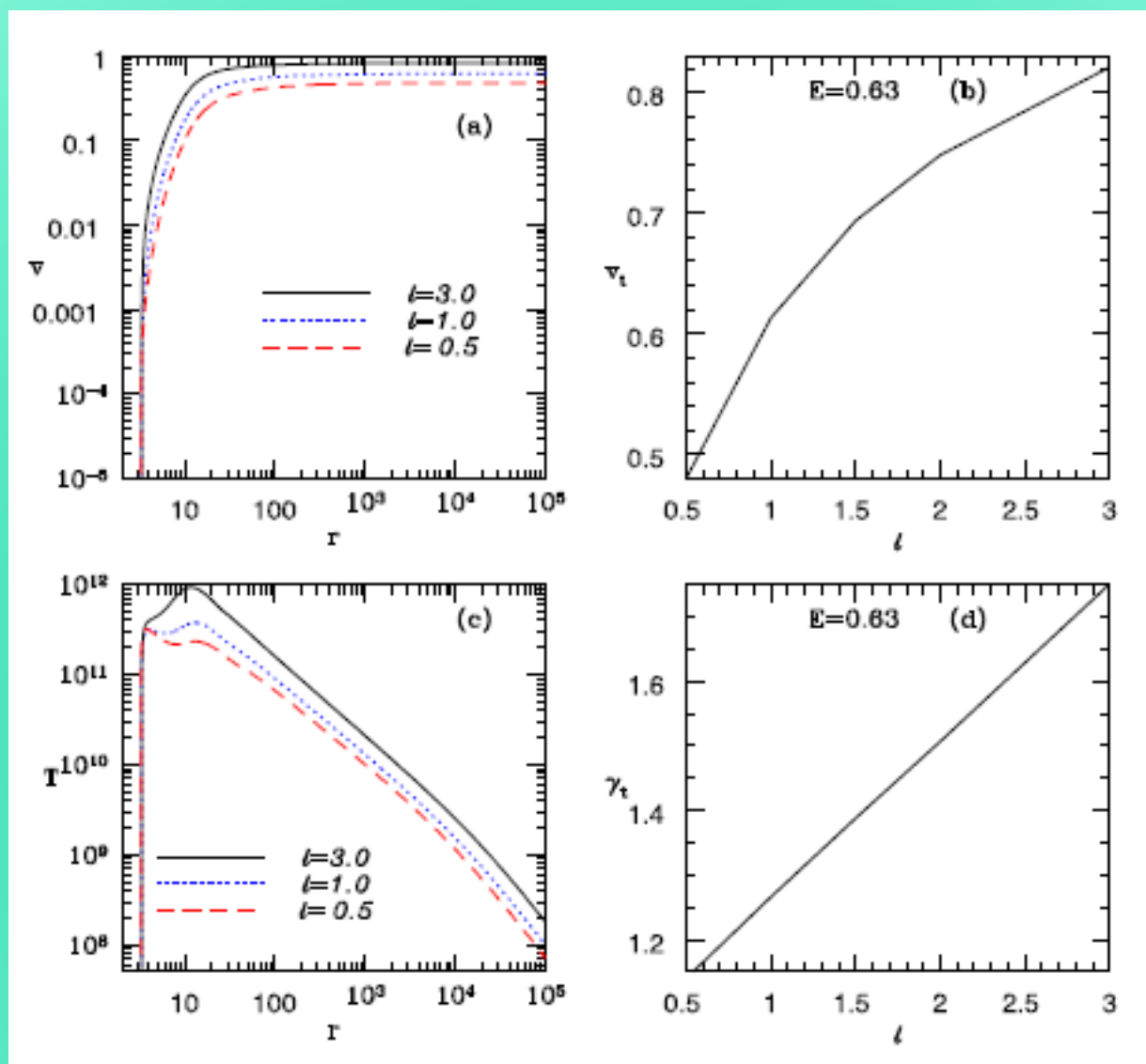


Figure 6. Nature of B-type solutions. Variation of (a)  $v$  and (b)  $T$  with  $r$  for  $E = 0.83$  and  $l = 1.0$  (solid) and  $l = 0$  (dashed).

Bound matter can be driven out as jet

(Vyas & IC 2019)



**Figure 10.** (a) Velocity profiles for various luminosities for C-type solutions for  $e^- - p^+$  composition. Corresponding terminal speeds ( $v_t$ ) are plotted in (b). (c) Variation of  $T$  with  $r$  for various luminosities. (d) Lorentz factor ( $\gamma_t$ ) as a function of  $\ell$  (solid). In panels (a) and (c), different curves are for  $\ell = 3.0$  (solid),  $\ell = 1.0$  (dotted) and  $\ell = 0.5$  (dashed), keeping  $E = 0.63$ .

(Vyas & IC 2019)

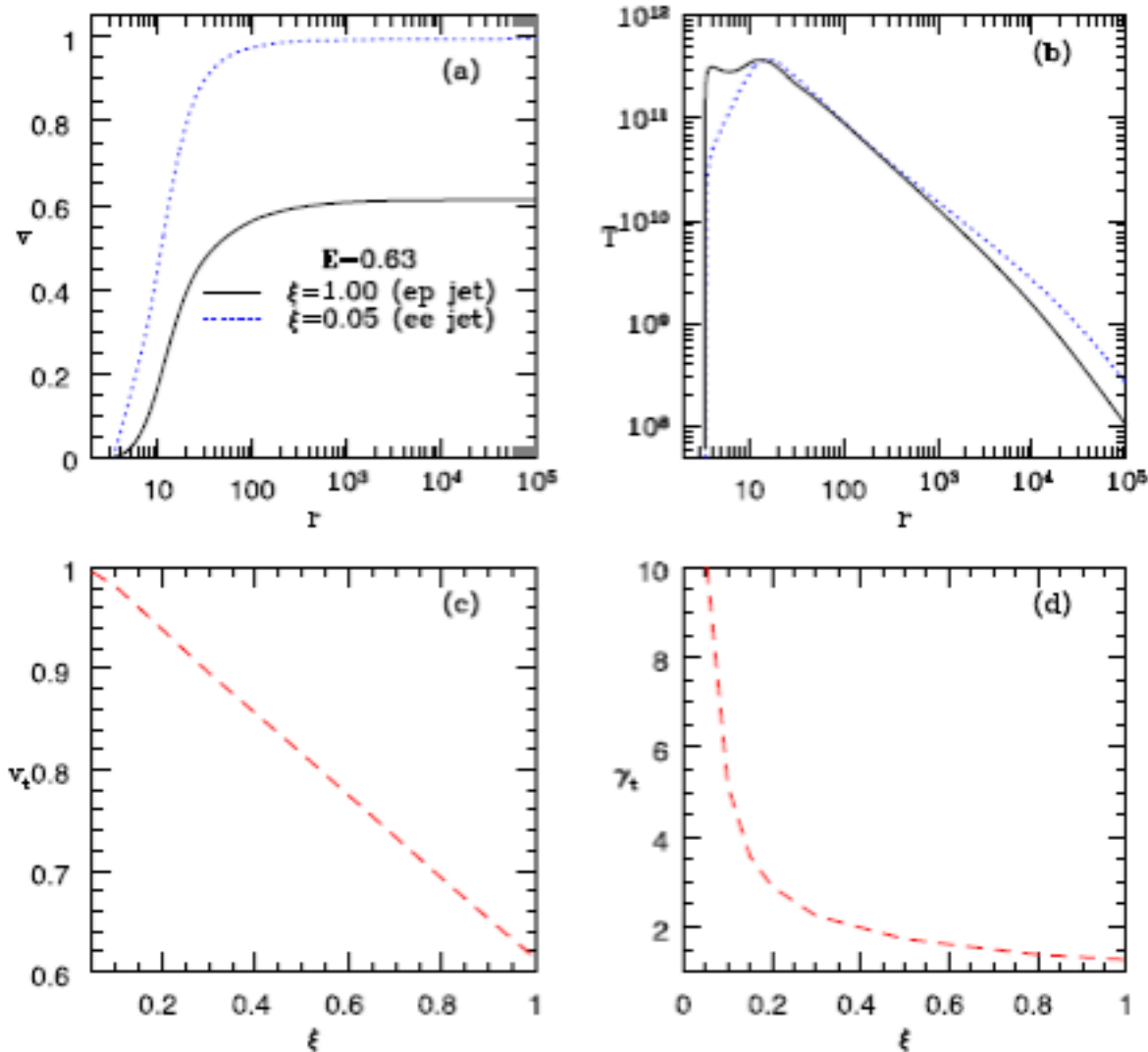


**Figure 11.** (a)  $v$  and (b)  $T$  profiles as a function of  $r$  for  $\xi = 0.05$  (dotted) and  $\xi = 1.00$  (solid). (c)  $v_t$  and (d)  $\gamma_t$  as a function of  $\xi$ . For all curves,  $E = 0.63$  and  $\ell = 1.0$ .

Compton scattering helps to obtain temperatures agreeable at the base, and yet reaching upto  $10^{12}$  K, at  $>10r_g$  above the disc.

Temperature of pair dominated flow may be similar to electron-proton jet, although much faster.

(Vyas & IC 2019)

## (II) Magnetically driven jet

### (a) Weber-Davis type wind:

(It is not a jet proto type of jet, but we would like study the effect of composition)

Eq. of motion

$$\nabla \cdot (\rho \mathbf{v}) = 0,$$

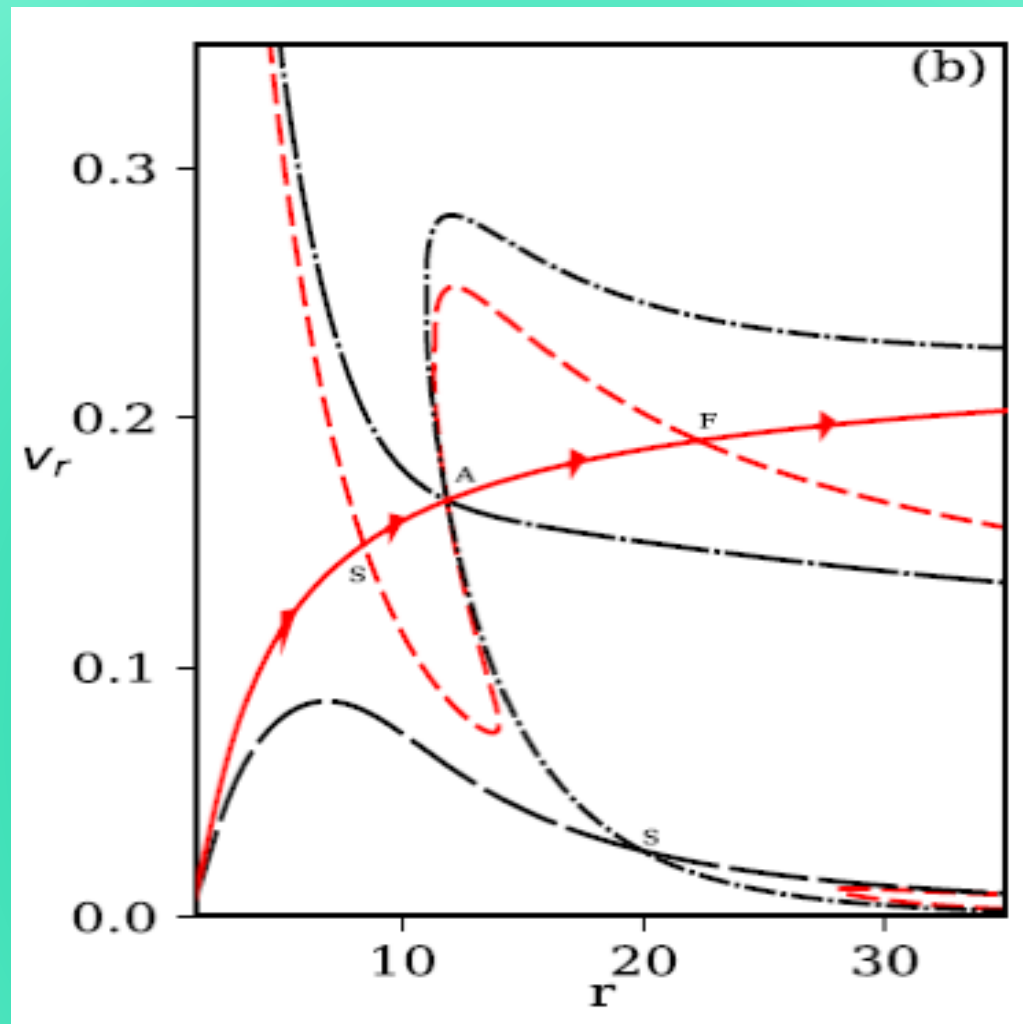
$$\nabla \cdot \mathbf{B} = 0,$$

$$\nabla \times (\mathbf{v} \times \mathbf{B}) = 0,$$

$$(\rho \mathbf{v} \cdot \nabla) \mathbf{v} = -\nabla p + \frac{1}{c} (\mathbf{J} \times \mathbf{B}) - \Phi'(r) \hat{r}.$$

Adiabatic relation  
with CR EoS

$$\mathcal{M} = \frac{\dot{M}}{4\pi Q} = v_r r^2 \exp(k_3) \Theta^{3/2} (3\Theta + 2)^{k_1} (3\Theta + 2/\eta)^{k_2}$$



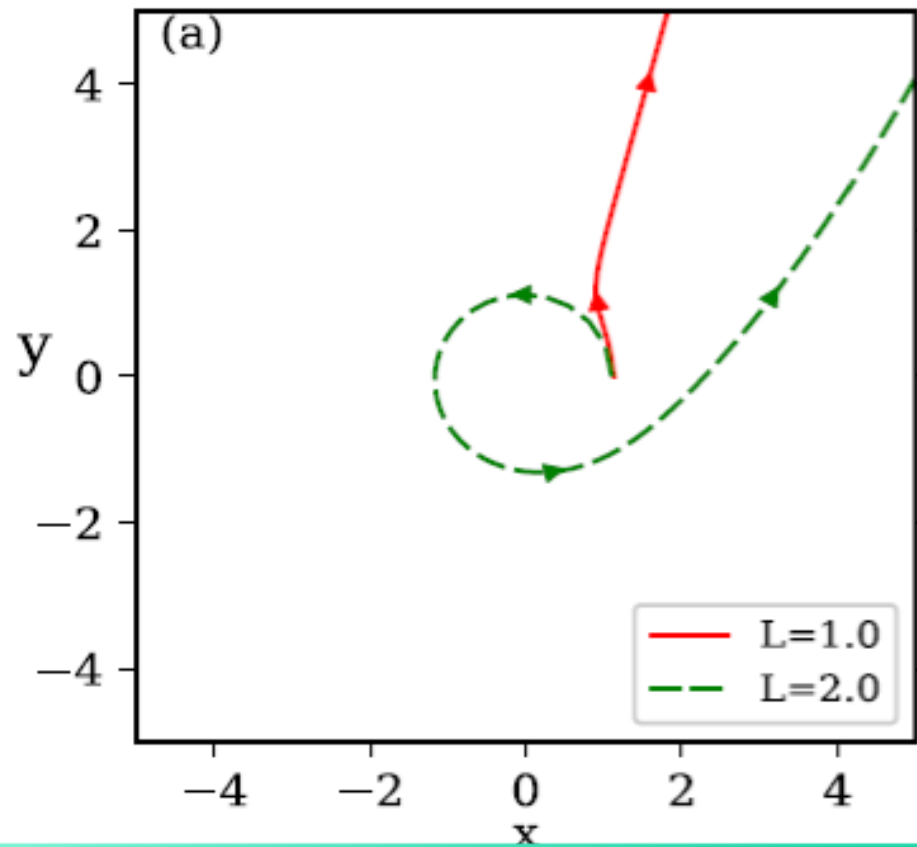
(Singh, IC, 2019)

(b)  $v_r$  versus  $r$  or actual outflow solutions. The solid (red) curve with arrow heads represents the transonic wind solution passing through slow, Alfvén and fast points, marked as S, A, and F, respectively. The dashed (red) curves are the transonic outflow solutions with wrong boundary condition. Long-dashed curve (black) is a trans-slow solution. Dash-dotted curve is the trans-slow, trans-Alfvén solutions and long-dash-dotted curve is a trans-Alfvénic flow.  $E = 1.04257$  (dotted, horizontal line),  $L = 1.75$  for all the curves.

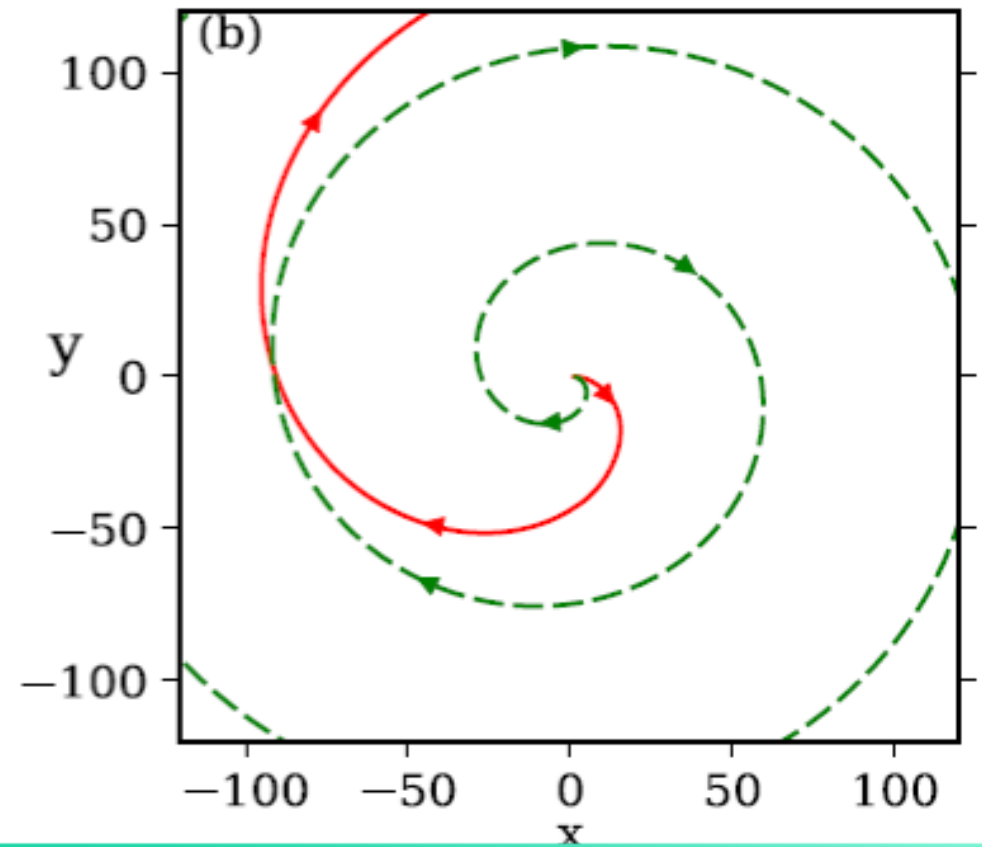
Passes through slow, Alfvén and fast points.

$$E = 1.03075.$$

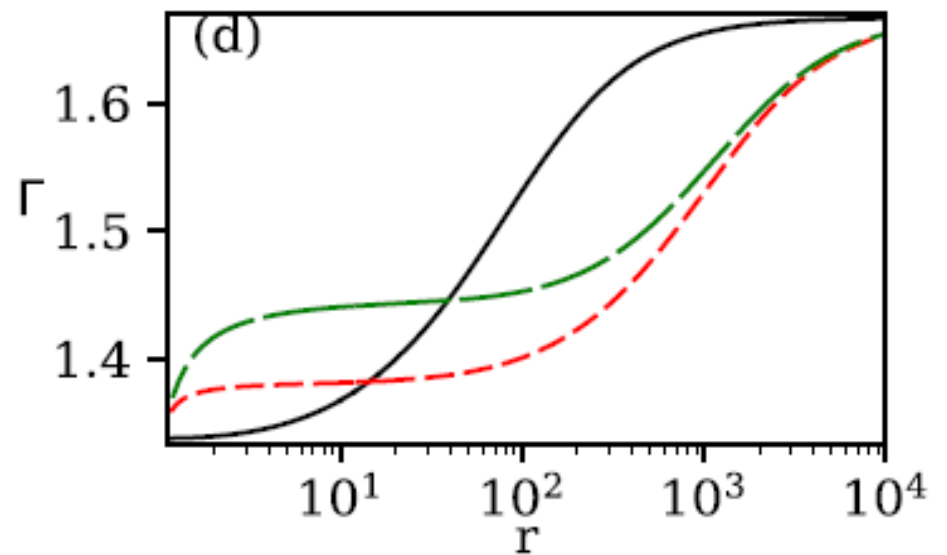
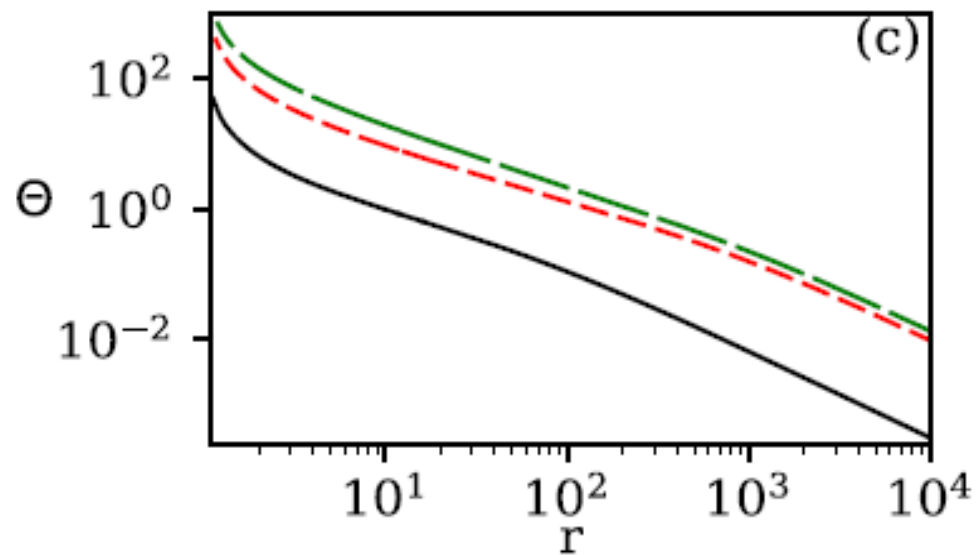
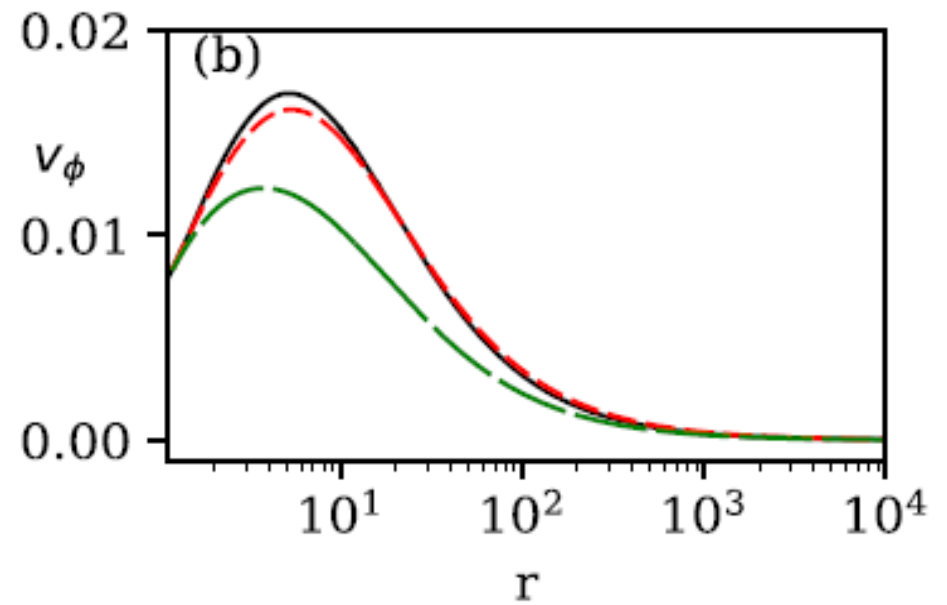
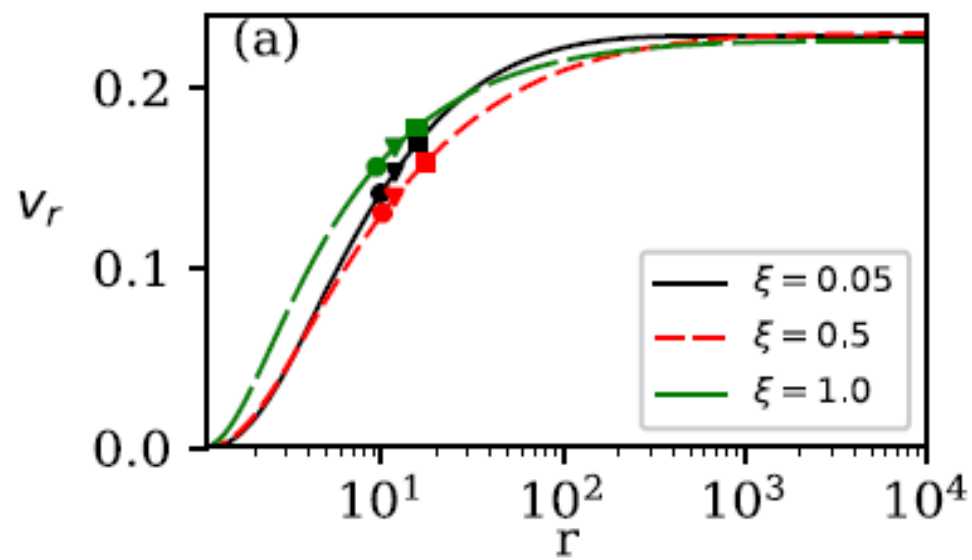
Stream Lines



Field Lines



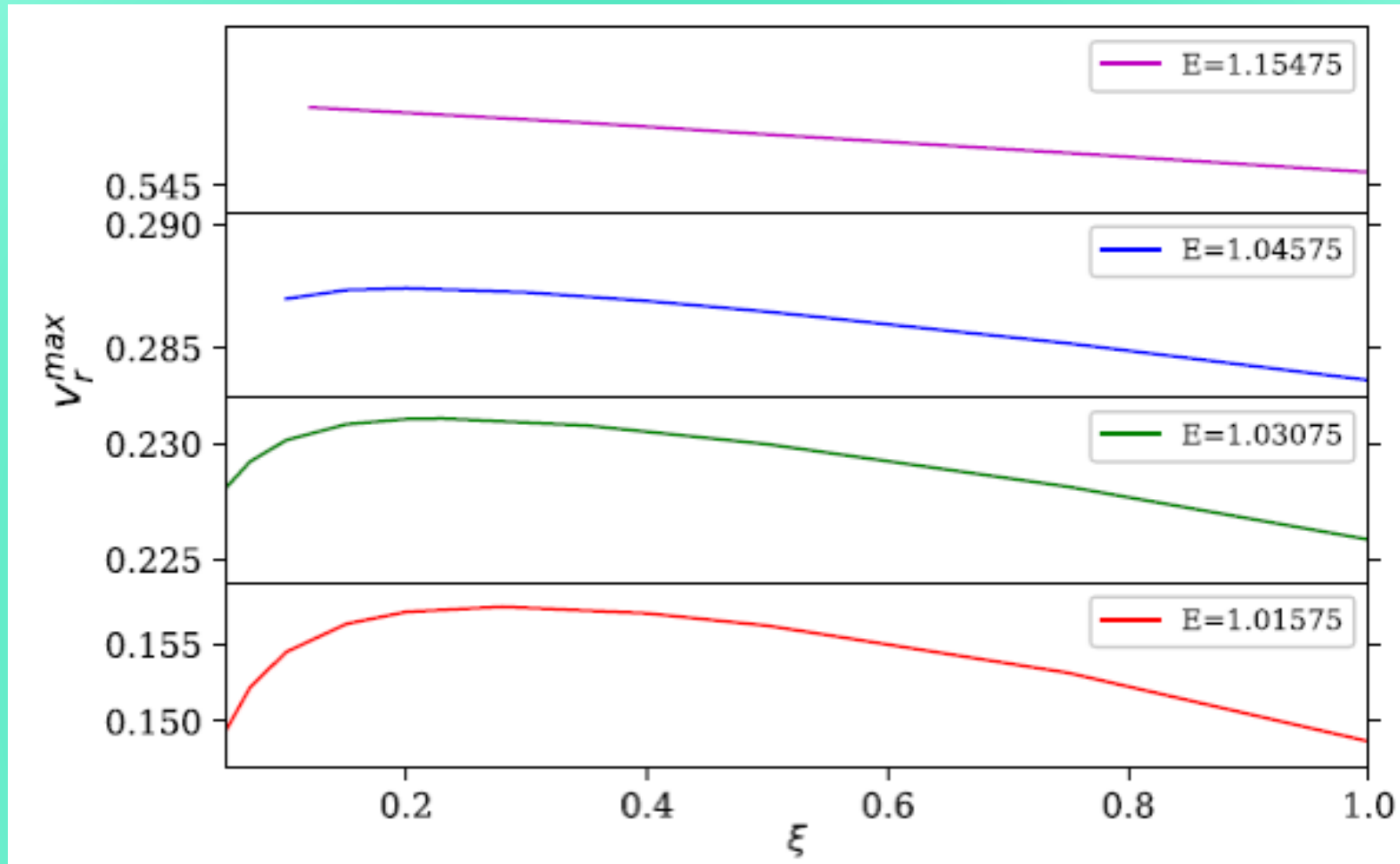
(Singh, IC,2019)



$E = 1.03075$  and  $L = 1.0$ .

(Singh, IC 2019)

$$L = 1.0$$



**Most significantly even the terminal speed depends on composition, unlike in the hydrodynamic limit.**

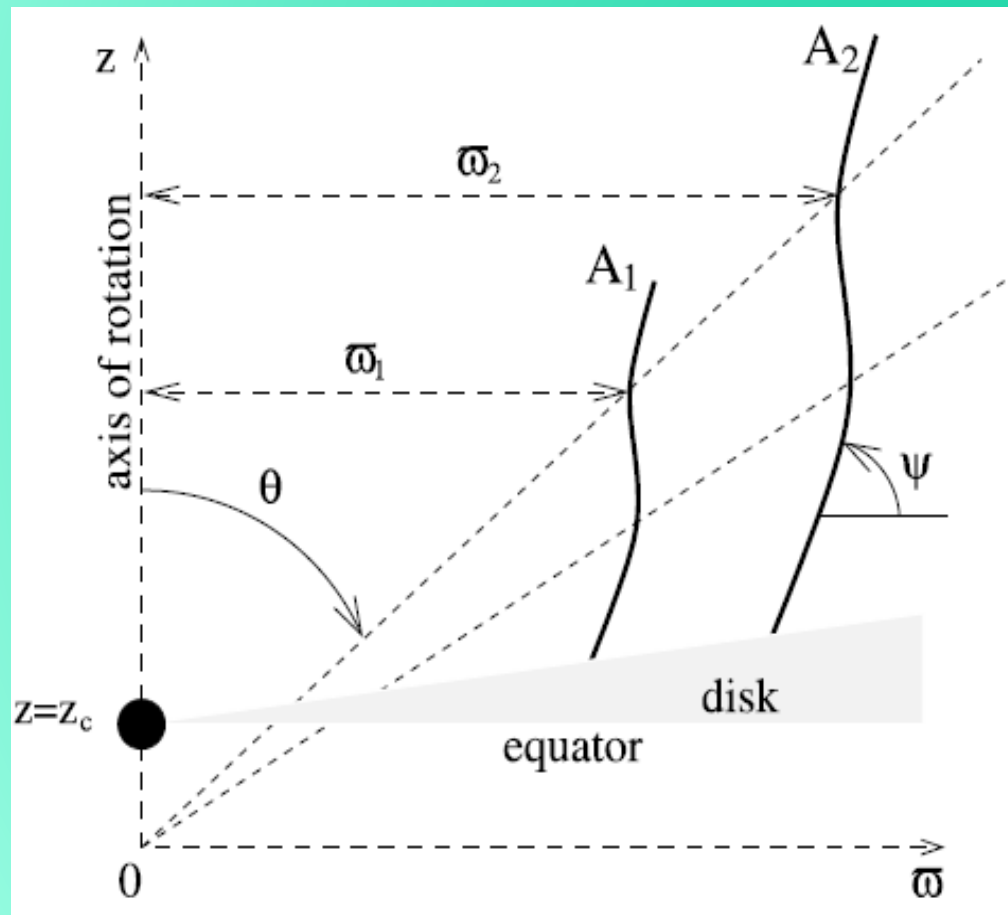
$$\frac{1}{2}v_r^2 + \frac{1}{2}v_\phi^2 + h + \Phi(r) - \frac{B_\phi B_r \Omega r}{4\pi \rho v_r} = \text{constant} = E$$

(Singh, IC 2019)

MHD winds, even as  $r \rightarrow \text{large}$ ,  $h \gtrsim 1$  because of the presence of the magnetic term and hence  $v_r^{\text{max}}$  depends on  $\xi$ .

## (b) Relativistic MHD outflow

FIG. 2.—Sketch of  $r$  self-similar field lines in the meridional plane. For any two field lines  $A_1$  and  $A_2$ , the ratio of cylindrical distances for points corresponding to a given value of  $\theta$  is the same for all the cones  $\theta = \text{const}$ :  $\varpi_1/\varpi_2 = (\alpha_1/\alpha_2)^{1/2}$ .



$$\frac{\partial(\gamma\rho)}{\partial t} + \nabla \cdot (\mathbf{v}\gamma\rho) = 0.$$

$$\gamma\rho \left( \frac{\partial}{\partial t} + \mathbf{v} \cdot \nabla \right) (h\gamma\mathbf{v}) = -\nabla p + \frac{J^0 \mathbf{E} + \mathbf{J} \times \mathbf{B}}{c}$$

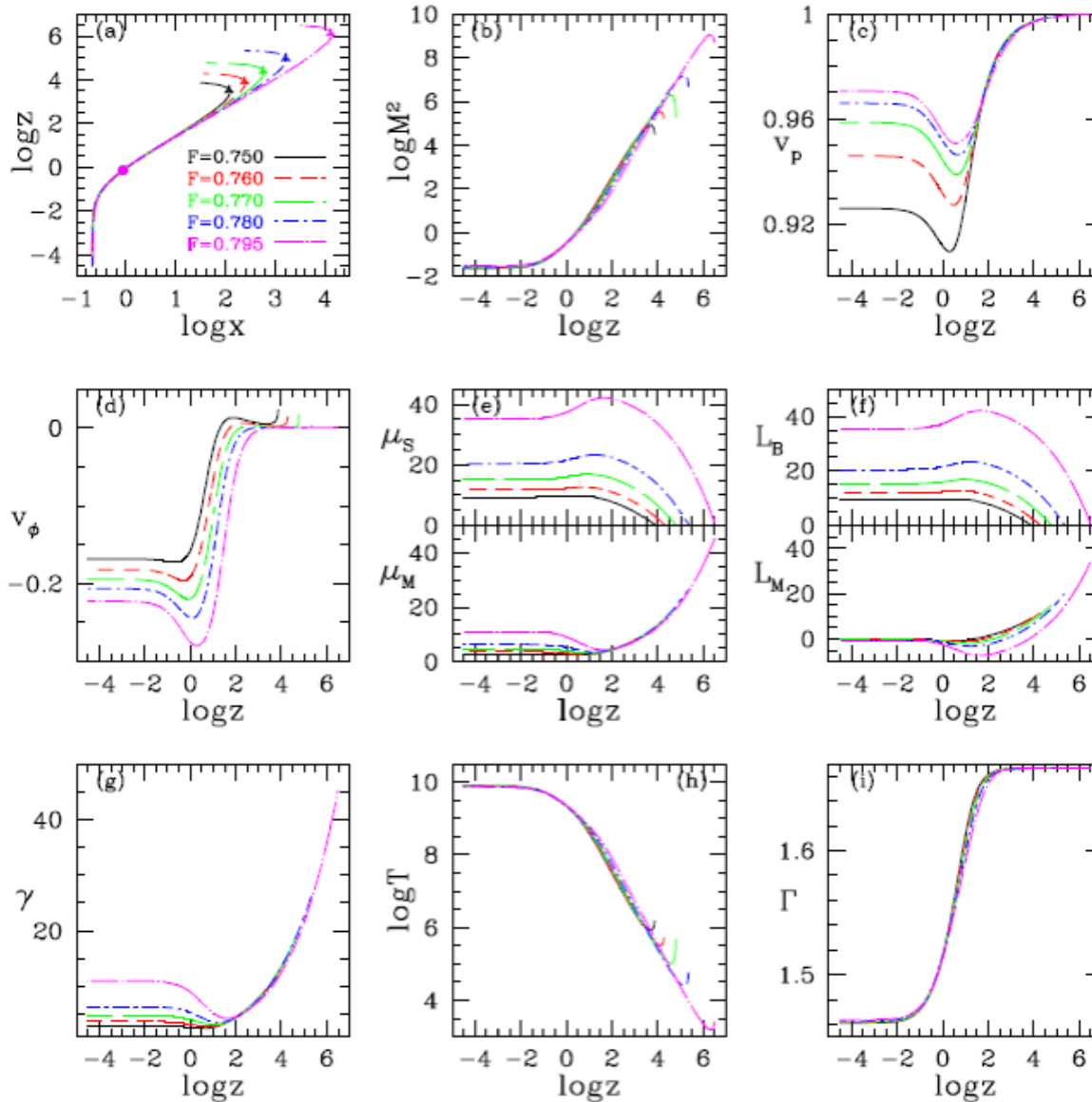
$$\left( \frac{\partial}{\partial t} + \mathbf{v} \cdot \nabla \right) e + p \left( \frac{\partial}{\partial t} + \mathbf{v} \cdot \nabla \right) \left( \frac{1}{\rho} \right) = 0$$

$$\partial/\partial t = 0 \text{ and } \partial/\partial\phi = 0$$

+ CR EoS

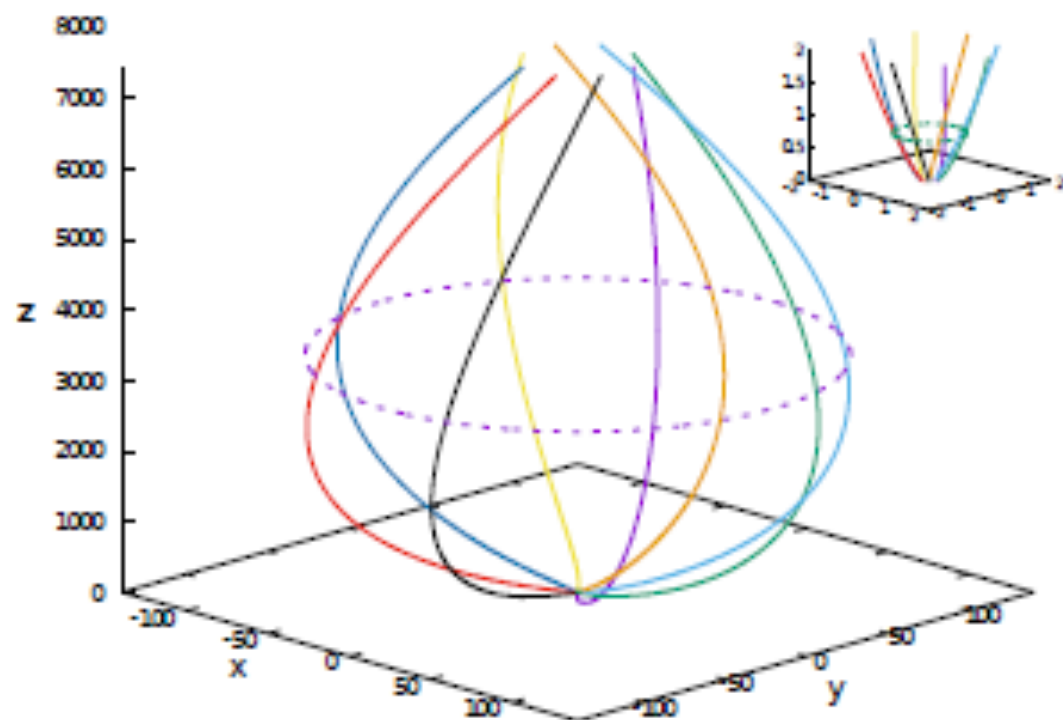
$$\mathbf{B} = \mathbf{B}_p + \mathbf{B}_\phi, \quad \text{where, } \mathbf{B}_p = \frac{\nabla A \times \hat{\phi}}{\varpi}$$

$$\mathbf{E} = \frac{\varpi\Omega}{c}\mathbf{B} \times \mathbf{e}_\phi, \quad \mathbf{v} = \frac{\Psi_A}{4\pi\gamma\rho}\mathbf{B} + \varpi\Omega\mathbf{e}_\phi \quad \text{and} \quad \frac{\Psi_A}{4\pi\gamma\rho} = \frac{v_p}{B_p}$$

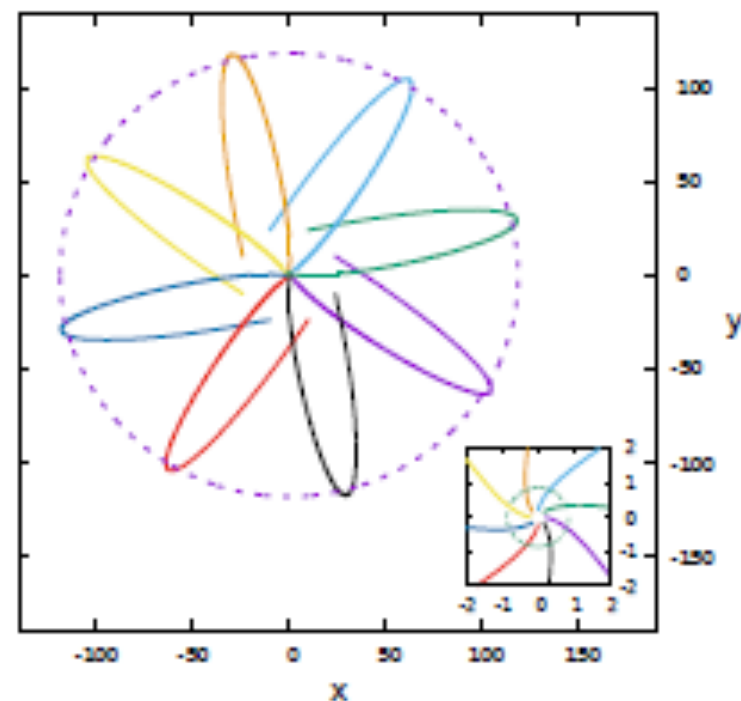


The flow passes through both Alfvén and fast points

(Singh, IC, submitted)



(a) Streamline side view.



(b) Streamline top view.

**Figure 2.** Solid lines represent the stream lines of outflow solution for  $x_A^2 = 0.75, \theta_A = 50, \psi_A = 55, F = 0.75, q = 500, \xi = 1$ . (a) Sideview and (b) top view. There are two dashed circles, one near to the center at  $z \sim 0.73$  represents the Alfvén point location and second at  $z \sim 3500$  represents the fast point location. Here,  $z$  is vertical height and  $x, y$  are in terms of light cylinder. Inset: Region close to the base is zoomed to show the location of the Alfvén point (dashed circle).

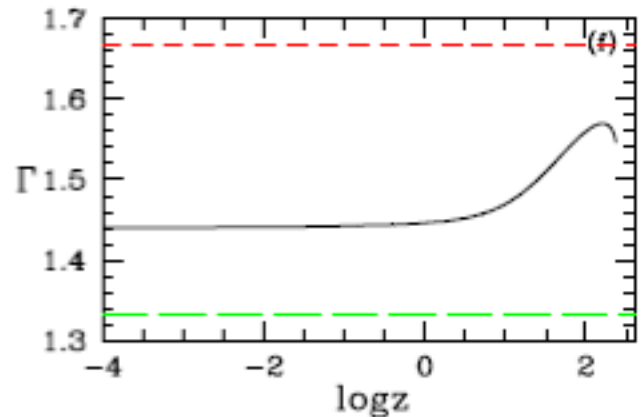
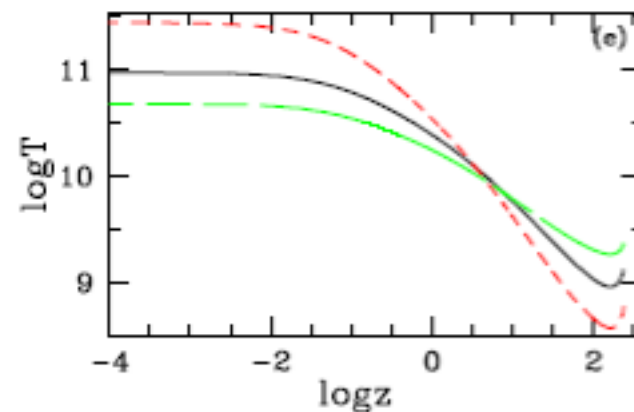
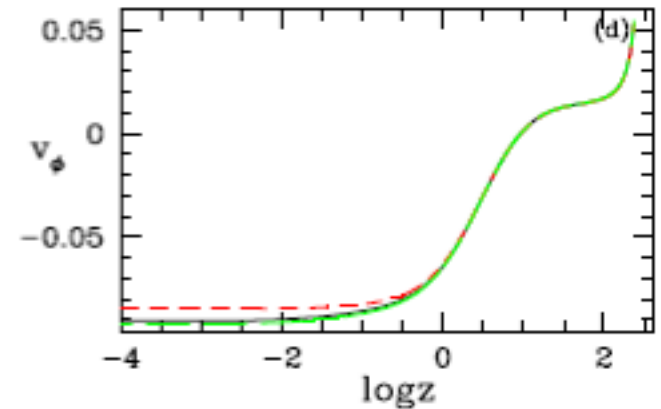
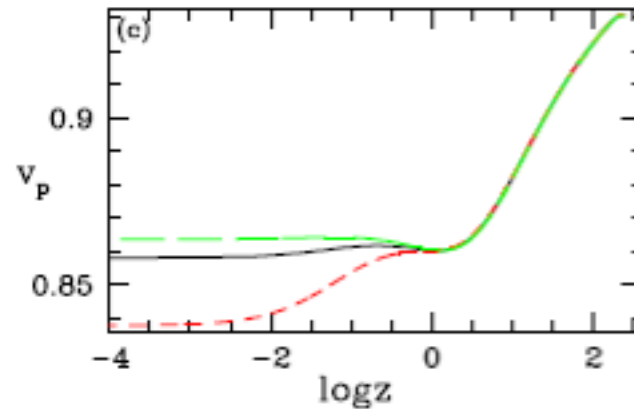
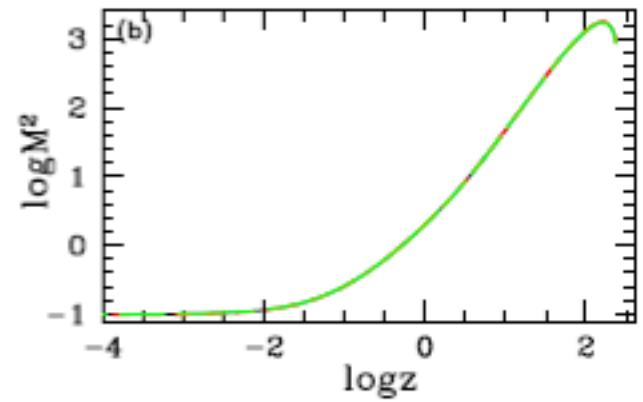
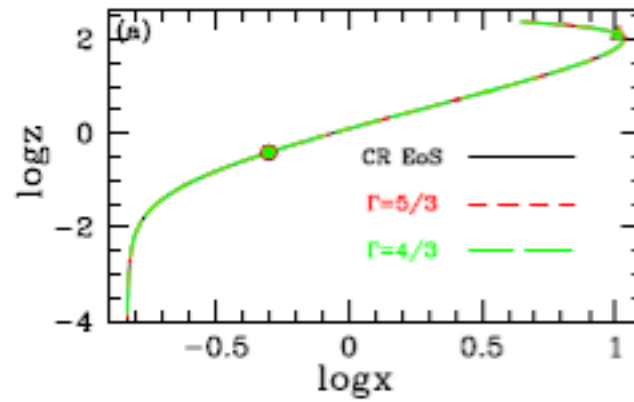
Azimuthal vel. Flips sign...

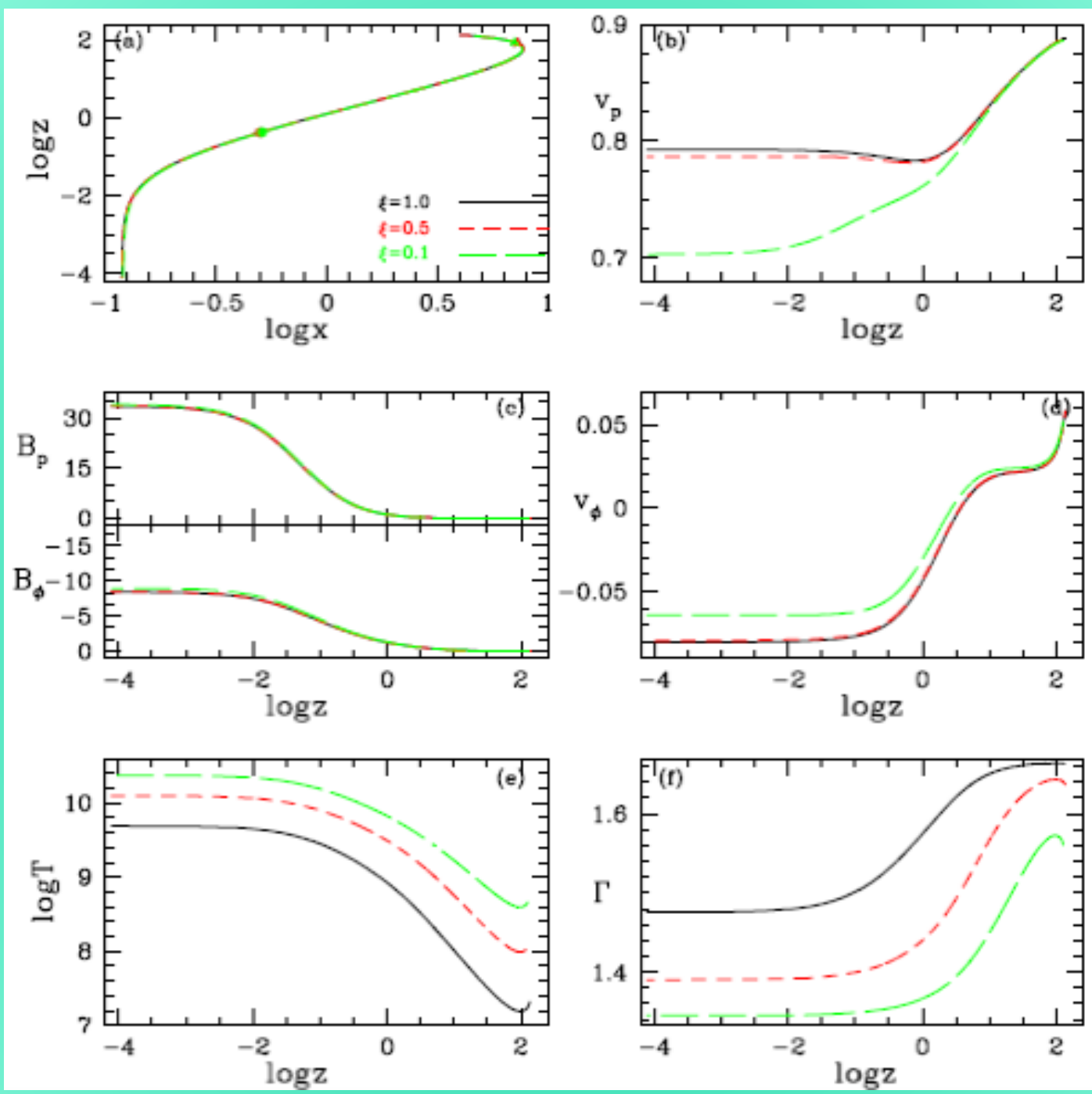
(Singh, IC submitted)

# Comparison with different EoS

No difference in streamline, but  $v_p$ ,  $T$ ,  $v$  are all different

(Singh, IC, submitted)



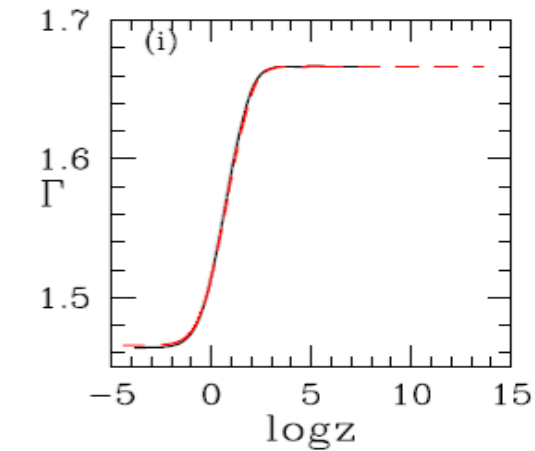
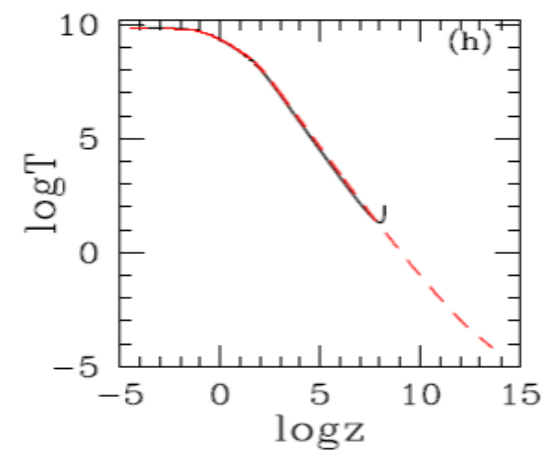
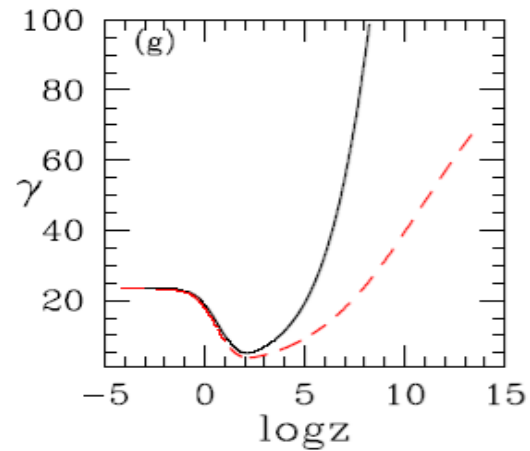
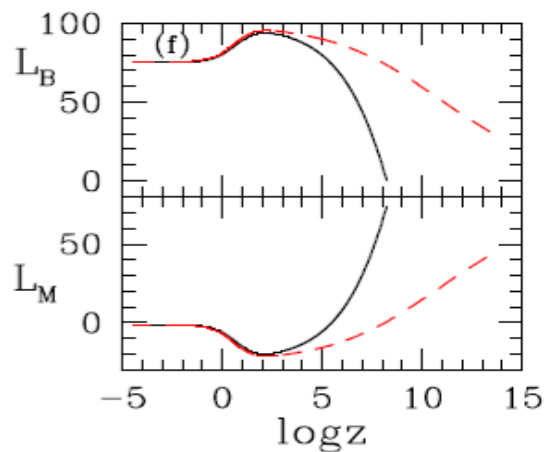
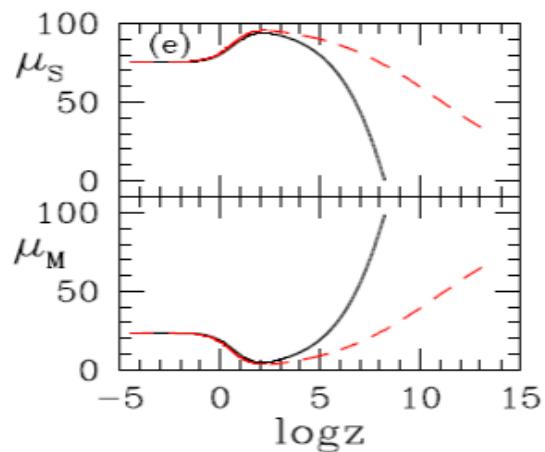
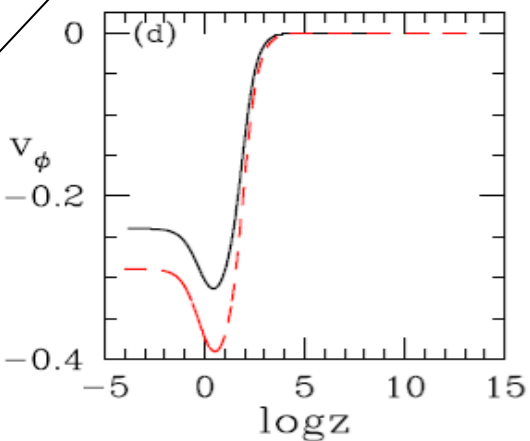
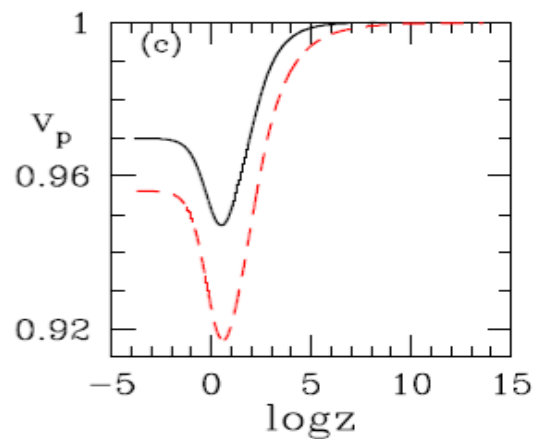
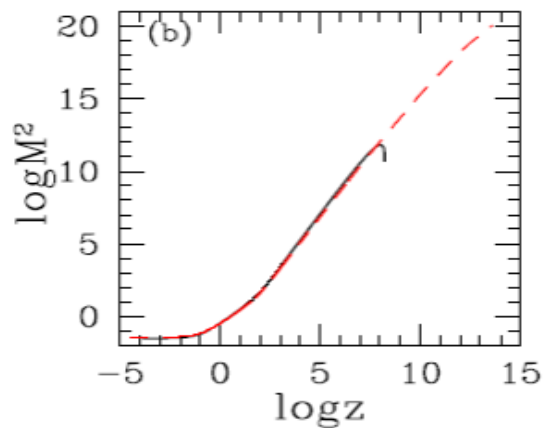
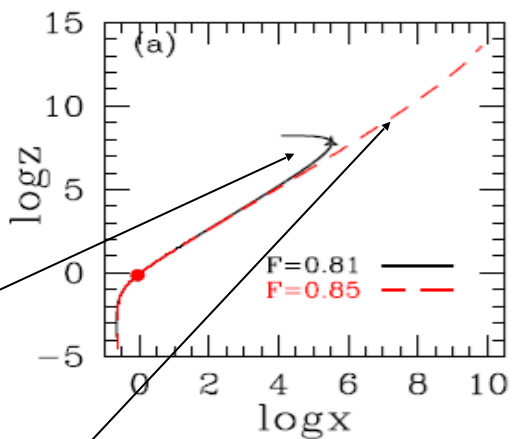


$\mu = 2.23362$ ,  $\theta_A = 50$ ,  $\psi_A = 55$ ,  $F = 0.75$ , and  $q = 500$ .

(Singh, IC, submitted)

Over-collimated

Not Over-collimated



## Conclusion:

- (i) Sufficiently luminous discs can accelerate jets to relativistic speed. Pair dominated flow can be accelerated to ultra-relativistic speed.
- (ii) To correct the temperature profile one need to consider Compton scattering.
- (iii) Magnetically driven outflows can achieve relativistic speed for both electron-proton, as well as, pair dominated flow.
- (iv) However, flows passing through the three critical points are always over collimated, while the one passing through only Alfvén point, extends up to large distance.
- (v) Radial self similarity needs to be re-looked, inclusion of gravity causes streamlines to cross.

Thank You